Sreedhar UNNIKRISHNAKURUP[1], C. V. Krishnamurthy[2], Krishnan BALASUBRAMANIAM[1]

CNDE, Mechanical Engineering Department, Indian Institute of Technology Madras, Chennai 600036 (1)
Department of Physics, Indian Institute of Technology Madras, Chennai 600036 (2)

doi:10.15199/48.2016.04.02

Monitoring TIG welding using infrared thermography – simulations and experiments

Abstract. *In the current work a 3D model has been developed to predict the thermal cycles during the Tungsten Inert Gas welding of Aluminum 2219. This paper describes the step by step procedure adopted to get the actual cooling rate during the TIG welding process both experimentally and numerically. The model was developed in the COMSOL Finite Element Package and considered a Gaussian heat distribution. The developed model then validated using the experimental data collected in field experiments on actual large propellant tanks. Temperature measurements were performed using Infrared Camera. Results show a close comparison between model and experiment.*

Streszczenie. *W pracy opracowano model 3D do przewidywania cykli cieplnych podczas spawania Aluminum 2219 z nietopliwą elektrodą wolframową w osłonie gazów obojętnych. Artykuł prezentuje krok po kroku przyjętą procedurę określania właściwego tempa chłodzenia (w eksperymencie jak i w modelowaniu numerycznym) podczas spawania. Model został stworzony w programie Comsol z gaussowskim rozkładem ciepła. Model numeryczny został porównany z danymi eksperymentalnymi. Pomiary temperatury wykonywano z użyciem kamery na podczerwień. Otrzymane wyniki pokazują dobrą zbieżność modelu z eksperymentem. (**Monitorowanie spawania z nietopliwą elektrodą wolframową w osłonie gazów obojętnych z użyciem termografii – symulacje i eksperymenty**).*

Keywords: Infrared Thermography, Online Monitoring, Finite Element Method, Image Analysis.
Słowa kluczowe: Termografia podczerwona, monitoring ciągły, metoda elementów skończonych, analiza obrazu.

Introduction

Fusion welding is a joining process that involves the phase change of materials. These processes are widely used in many engineering applications such as aerospace, automotive and ship building industries. A good quality weld is characterized by material composition, joint condition, relative position of the welding arc to the joint and welding parameters such as arc current, arc voltage and torch travel speed. Therefore choosing an appropriate set of welding parameters becomes one of the most important tasks in TIG welding process. In the current industrial practice welding processes are developed largely based on trial and error experiments incorporating with engineer's knowledge and experience of previous similar designs. So it is very important to identify and optimize various welding parameters and thereby control the process for the defect free manufacturing [1].

Arc welding is inherently a thermal processing method. To this end, infrared sensing is a natural choice for weld process monitoring. Infrared sensing is the non contact measurement of emissions in the infrared portion of the electromagnetic spectrum. Many investigators have used thermographic system for the measurement of temperature distribution and control of welding online [2–6]. Most of these measurements are reported from the weld pool region. In the current study we explored the monitoring of solidified weld region just after the weld torch passes. This online measurement technique is well utilized for the defect identification during welding process [7].

The various transport phenomena in the weld pool directly affect the size and shape of the weld formed, solidification microstructure, the formation of the weld defects such as porosity and humping, and the temperature distribution in the fusion zone and heat affected zone. Simulation tools based on finite element method are very useful in the prediction of temperature fields in welding. Owing to the growing needs of automation and better weld quality control there have been several attempts to model the actual welding phenomena by considering all the physics involved in the weld pool [8–14]. All these models require the specification of net thermal input from the welding arc to the work piece along with its spatial distribution. The research on welding heat source models dates back 1940s and Rosenthal first proposed a mathematical model of the moving heat source under the assumptions quasi-stationary state and concentrated point heating in the 3D analysis [15]. In the late 1960s, Pavelec et al. suggested a circular disc heat source model with Gaussian distribution of heat flux on the surface of work piece. Goldak et al. further developed a double ellipsoidal power density distribution of heat source model below the welding arc, which can accurately simulate different type of welding processes with shallow and deep penetration [16]. These heat source models and some simplified models have been widely used in welding simulation for prediction of temperature field, distortion and the residual stresses.

In the current study to simulate the heat flux from the arc we used the Gaussian heat distribution because of the consideration that less heat flux penetration is involved in arc welding process than the high power density welding processes(EBW and LBW), where the double ellipsoidal model can capture the flux penetration effectively.

Modeling and Simulations

Mathematical and Numerical Model

Both 2D and 3D heat conduction models were developed to simulate the TIG welding process. The developed models consider a moving heat source along the Aluminum plate. The thickness of the plate is given in the thickness axis and is positive toward the upper side. The weld path is defined at the center as a separate surface. The heat source will move over this surface along the positive x direction with a constant velocity v. As a result of the heat input a molten pool will create under the heat source. In the current study we assume that the material is homogeneous and thermo physical properties are constant also the formation of molten pool and the forces acting in the weld pool are not considered. The details of our 2D modeling part is published earlier and is available online [17]. For a three-dimensional unsteady state heat transfer in the isotropic welding plate without any heat generation, the governing equation can be expressed as follows:

$$\frac{\partial}{\partial x}\left(k\frac{\partial T}{\partial x}\right)+\frac{\partial}{\partial y}\left(k\frac{\partial T}{\partial y}\right)+\frac{\partial}{\partial z}\left(k\frac{\partial T}{\partial z}\right)=\rho c\left(\frac{\partial T}{\partial t}\right) \quad (1)$$

Where T determines the temperature of the plate, k thermal conductivity, ρ is the density of the plate, c is specific heat and t represent the time duration. The convective and radiative boundary heat losses were considered and it is represented as follows:

$$n.(k\nabla T) = Q + h(T_{\inf} - T) + C_{const}\left(T_{amb}{}^4 - T^4\right) \quad (2)$$

Where Q is the inward heat input from electric arc is, h is the convective heat transfer coefficient, n is the vector normal to the surface. The welding arc heat source is considered as a distributed boundary heat source. The weld path is defined as a boundary in the geometry and the heat source term is expressed as a boundary expression in the model. The Gaussian heat source model is defined as follows:

$$Q = \frac{3\eta VI}{\pi r_b{}^2} e^{\frac{-3\left[(x-x_0)^2+(y-y_{fl})^2\right]}{r_b{}^2}} \quad (3)$$

Where η is the arc efficiency, V and I are voltage and current values, r_b represents the Gaussian base radius and x_0 and y_{fl} are coordinate points to locate and define the motion of the weld torch along the weld path. The coordinate point y_{fl} is given by $v*t$, where v is the velocity of the weld torch and t is the welding time. The initial condition is assumed as ambient temperature 300K.

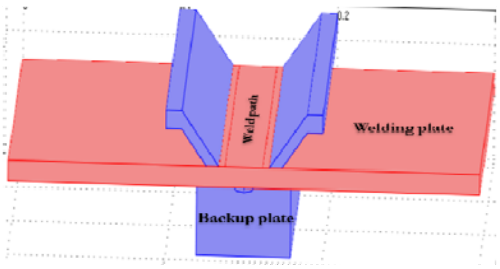

Fig. 1. 3D Model geometry

Solution

The model corresponding to the production field experiment is also constructed using COMSOL GUI interface. The model considered all the fixtures and clamps used for the actual experiment. Fig. 1 shows the model geometry used for the temperature simulation. A tight contact is assumed for butt welding of the two cylinders and due to the larger diameter of the cylinder, the numerical model considers only the straight plates. A very fine meshing is used for the weld path, where the high thermal gradients are present.

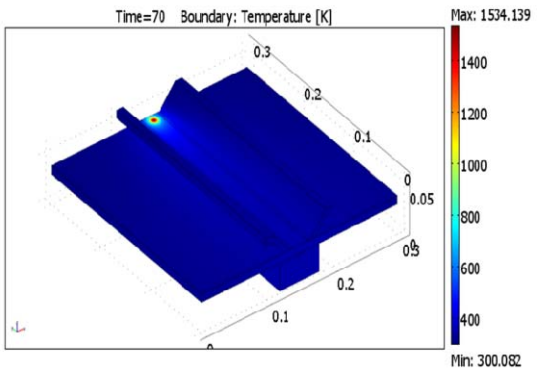

Fig. 2. Temperature distribution in the plate at the end of heating

Fig. 2 shows the surface plot of temperature for the 3D FEM simulation problem after 70s. This simulation corresponds to the actual field measurement data. Here the distributed Gaussian heat source moves from one end of the plate to the other end with a constant speed. The temperature distribution in the plate due to the arc heating, heat exchange between the back up plates and the holding clamp and the heat transport due to convection and radiation were modeled using the present model.

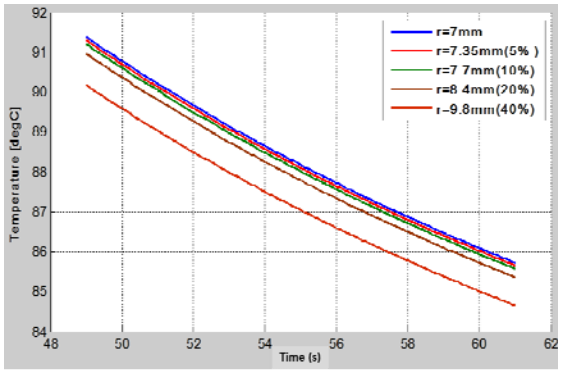

Fig. 3. Variation of temperature distribution for different heat source radius

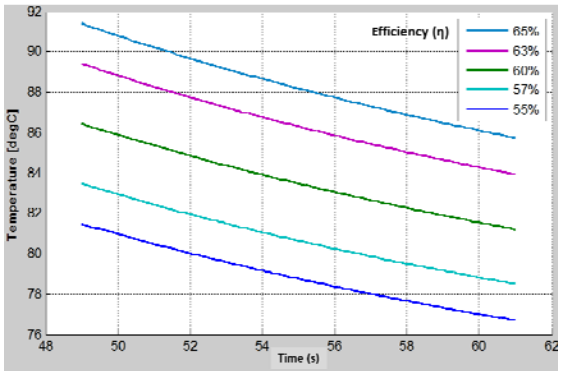

Fig. 4. Variation of temperature distribution with heat source efficiency

The temperature data were analyzed at distance of 150 mm behind the heat source center in order to match the actual experimental measurements. Fig. 3 and
Fig. 4 show the distribution of temperatures for different welding conditions. These cooling curves correspond to the experimentally measured data. Fig. 3 shows the spread in temperature values with respect to the Gaussian radius, which depends on other welding variables such as current, voltage and the arc length. It is observed that a 40% increase in the base radius resulted only 1% variation in the temperature profiles.

Fig. 4 corresponds to the spread due to the variation in welding efficiency, which again a dependant variable of welding parameters. It is observed from this parametric study on the efficiency value, a 10% variation in the efficiency resulted in 12% variation in the corresponding thermal cycles. From this 3D numerical model for the no defect region it is clear that the spread in the experimental data is due to the variation in these control variables and the varying boundary condition.

Experimental Study

A circumferential welding was carried out between shell and dome structure of AA2219 propellant tank using a automatic TIG welding machine in a manufacturing plant. This welding joins the shell and the dome structure of a propellant tank of 4 m diameter and 9 mm thick weld line region. The infrared camera mounted at certain angle to the weld plate on the welding torch arm. IR Camera was tied on the arm of the weld torch as shown in

Fig. . The welding was carried out in two passes. The first pass was welded autogenously and in the second pass AA 2213 was used as filler wire. The IR camera was

focused to an area 150 mm away from the weld torch as shown in Fig. . The length along the weld the camera sees was about 100 mm. This measurement system is adopted after several feasibility studies in order to avoid the saturation of detector due to the high temperature infrared emissions near the weld pool region.

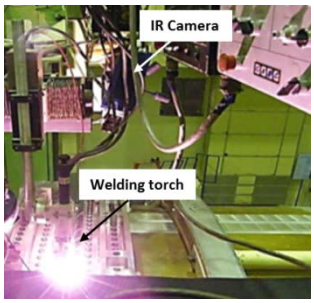

Fig. 5. Experimental set up of shell to dome TIG welding

The thermal image obtained during the experiment is shown in Fig. . The infrared camera obtains thermal maps called thermographs from the distribution and a custom built interface transfers these images from the camera to the computer for further analysis. The thermal image obtained during the welding process at a certain tank location.

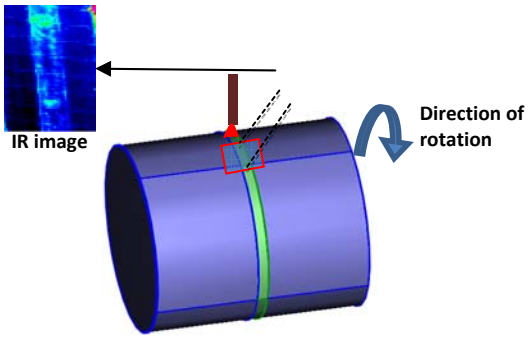

Fig. 6. Schematic of experimental set up showing the field of view of the measurement

Due to the tilted camera the finger clamps used for the fixture is also present in the thermal image. Steel is used as finger clamps. From the thermal image it is observed that the finger clamps were at a high temperature compared to the AA 2219 weld region. The reason is the FOV is away from the weld torch and because of that the aluminum gets cool fast and the steel get heated up. Due to the low thermal conductivity of steel it is showing a high temperature compared to aluminum.

Image analyzing algorithms were developed to find the transient temperature decay data from the raw thermal images in which the material is moving. A more detailed account of the procedure is highlighted in Fig. [7]. The cooling rate of a point at the center of the weld bead is measured using the algorithm and the measurements were taken at different locations of the welded cylinder. The material is moving through the field of view. Each pixel area on the material stays only for 12 seconds in the field of view. This was found out using the tracking of points from the experimental data at different locations. The algorithm has taken care of the welding speed, frame rate at which the thermal images were taken and the horizontal pixel position. The point plot in Fig. corresponds to the cooling rate at different locations and the dotted line is the average value of the measured experimental data.

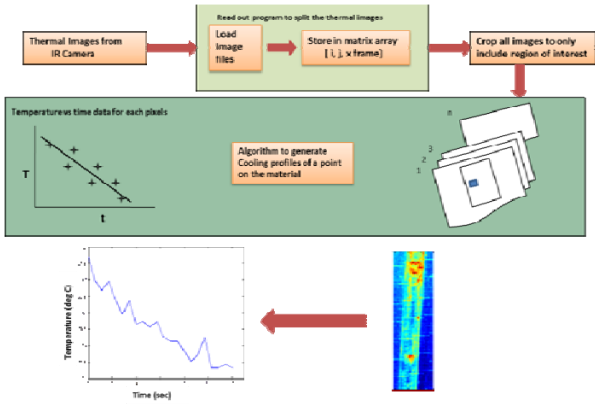

Fig. 7. Flow diagram details of the time-temperature profile generation

Results and Conclusion

Fig. shows the temperature decay curves obtained from the 2D and 3D models and from the experimental data. In the experimental data, a spread in the data can be observed from the graph. These were data points measured at different no-defect locations of the welded tank. Also an average of all these data point is also plotted. In the 2D model the temperature history is taken by considering the time duration needed for the material to reach the field of view. Both 2D and 3D model results showed a very close matching in the temperature history. The variation in the 2D and 3D models is due to the difference in the assumed heat input parameters. In 2D these parameters are optimized using the experiment.

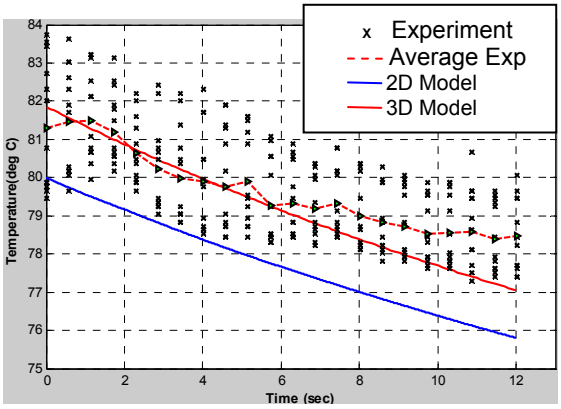

Fig. 8. Comparison of cooling curves for experiment and simulation

A numerical model of the TIG welding process to perform simulation of the surface thermograms is developed using the finite element method and implemented it using the commercial software COMSOL Multiphysics. The validation of the 2D and 3D models were carried out using the experimental data collected in field experiments on actual large propellant tanks. The simplified 2D model developed initially, with a heat source that was optimized using the experiment, gave a close comparison with the experimental data in the entire non-defective region. The development of the 3D simulation model for the non defective weld case with the Gaussian heat source parameters gives a close comparison with the experiment. The spread of experimental data in the non defective region is verified by the variation of weld process parameters. The parametric study shows that the Gaussian heat source radius is less sensitive to the temperature variation in the observed region but the efficiency values are considerably sensitive to the temperature changes. It is well known from the earlier studies that the heat flow which is away from the

heat source is only affected by the total amount of energy deposited on the material, which is controlled by the efficiency value and the distribution is not important in determining the temperature distribution away from the source as observed for Gaussian base radius.

Acknowledgment: This work was financially supported by Indian Space Research Organization, India, under the project entitled Development of an Online Weld Defect Characterization using Thermal Imaging Techniques.

***Authors**: Sreedhar U, IITM, sreedhar.aie@gmail.com, C. V. Krishnamurthy, IITM, cvkm@iitm.ac.in, K. Balasubramaniam, IITM, balas@iitm.ac.in*

REFERENCES

[1] D. A. Hartman, M. B. Science, and G. E. Cook, "Arc Welding Process Control," in *ASM Handbook 6A. Welding Fundamentals and Processes*, vol. 6, 2011, pp. 285–295.

[2] S. M. Govardhan, H. C. Wikle III, S. Nagarajan, and B. a. Chin, "Real-time welding process control using infrared sensing," *Proc. 1995 Am. Control Conf. - ACC'95*, vol. 3, pp. 1712–1716, 1995.

[3] T. G. Lim and H. S. Cho, "Estimation of weld pool sizes in GMA welding process using neural networks," vol. 207, 1993.

[4] H. Fan, N. Ravala, H. Wikleiii, and B. Chin, "Low-cost infrared sensing system for monitoring the welding process in the presence of plate inclination angle," *J. Mater. Process. Technol.*, vol. 140, no. 1–3, pp. 668–675, 2003.

[5] R. S. Huang, L. M. Liu, and G. Song, "Infrared temperature measurement and interference analysis of magnesium alloys in hybrid laser-TIG welding process," *Mater. Sci. Eng. A*, vol. 447, no. 1–2, pp. 239–243, 2007.

[6] N. M. Nandhitha, N. Manoharan, B. S. Rani, B. Venkataraman, P. K. Sundaram, and B. Raj, "Automatic Detection and Quantification of Incomplete Penetration in TIG Welding Through Segmentation and Morphological Image Processing of Thermographs," *Proc. Natl. Semin. Non-Destructive Eval. Dec. 7 - 9, 2006, Hyderabad*, pp. 17–22, 2006.

[7] U. Sreedhar, C. V. Krishnamurthy, K. Balasubramaniam, V. D. Raghupathy, and S. Ravisankar, "Automatic defect identification using thermal image analysis for online weld quality monitoring," *J. Mater. Process. Technol.*, vol. 212, no. 7, pp. 1557–1566, 2012.

[8] M. A. Wahab, M. J. Painter, and M. H. Davies, "The prediction of the temperature distribution and weld pool geometry in the gas metal arc welding process," *J. Mater. Process. Technol.*, vol. 77, no. 1–3, pp. 233–239, 1998.

[9] a. Mahrle, J. Schmidt, and D. Weiss, "Simulation of temperature fields in arc and beam welding," *Heat Mass Transf.*, vol. 36, no. 2, pp. 117–126, 2000.

[10] F. Lu, X. Tang, H. Yu, and S. Yao, "Numerical simulation on interaction between TIG welding arc and weld pool," *Comput. Mater. Sci.*, vol. 35, no. 4, pp. 458–465, 2006.

[11] M. Carin and E. Favre, "Numerical simulation of fluid flow during arc welding.," Comsol Conference, 2005.

[12] F. Lu, "Modeling and finite element analysis on GTAW arc and weld pool," *Comput. Mater. Sci.*, vol. 29, pp. 371–378, 2004.

[13] S. Kou and Y. Le, "Heat Flow during the Autogenous GTA Welding of Pipes," *Metall. Trans. A*, vol. 15, no. 6, pp. 1165–1171, 1984.

[14] E. a Bonifaz, "Finite Element Analysis of Heat Flow in Single-Pass Arc Welds," *Weld. J.*, pp. 121–125, 2000.

[15] C. L. Tsai and U. S. Design, "Heat Flow in Fusion Welding *," in *ASM Handbook 6A. Welding Fundamentals and Processes*, vol. 6, 2011, pp. 55–66.

[16] J. Goldak, A. Chakravarti, and M. Bibby, "A New Finite Element Model for Welding Heat Sources," vol. 15, no. June, pp. 299–305, 1984.

[17] U. Sreedhar, C. V Krishnamurthy, and K. Balasubramaniam, "Non-Destructive Evaluation Modeling and Simulation for Temperature Prediction in Welding Using Infrared Thermography," no. August 2015, pp. 396–400, 2009.